

Chaos and magnetospheric dynamics

G.P. Pavlos¹, D. Diamandidis¹, A. Adamopoulos², A.G. Rigas¹, I.A. Daglis³ and E.T. Sarris^{4*}

¹ Demokritos Univ. of Thrace, Dept. of Electr. Eng., Division of Telecommunications & Space Science, 67100 Xanthi, Greece

² Demokritos Univ. of Thrace, Dept. of Medicine, Medical Physics Laboratory, 68100 Alexandroupoli, Greece

³ Max-Planck-Institut für Aeronomie, 37189 Katlenburg-Lindau, Germany

⁴ National Observatory of Athens, Institute of Ionospheric and Space Research, 11810 Athens, Greece

Received 2 December 1993 - Accepted 24 March 1994 - Communicated by S. Lovejoy

Abstract. Our intention in this work is to show, by using two different methods, that magnetospheric dynamics reveal low dimensional chaos. In the first method we extend the chaotic analysis for the *AE* index time series by including singular value decomposition (SVD) analysis in combination with Theiler's test in order to discriminate dynamical chaos from self-affinity or "crinkliness". The estimated fractality of the *AE* index time series which is obtained belongs to a strange attractor structure with close returns in the reconstructed phase space. In the second method we extend the linear equivalent magnetospheric electric circuit to a nonlinear one, the arithmetic solution of which reveals low dimensional chaotic dynamics. Both methods strongly support the existence of low dimensional magnetospheric chaos.

et al., 1988). The importance of these concepts for magnetospheric physics can become apparent if we think the difficulty until now to obtain a global comprehension of the magnetospheric processes. Pavlos (1988) used the concept of system dynamical-state motion on a strange attractor as an explicative paradigm of magnetospheric substorms. It is helpful to present here a short part of this paper:

"...The magnetospheric system is open, as it exchanges mass and energy with the ionosphere and the solar wind, while it remains far from thermodynamic equilibrium. For this reason the magnetosphere belongs to the class of dissipative chaotic systems. An important consequence of chaos theory for these systems is the possibility of existence of strange attractors in phase space. Our failure until now to develop a sufficient, local-character description of magnetospheric dynamics, through not extinguishing the hope for future achievements, supports our suggestion that chaos theory may constitute a powerful tool for a global comprehension of magnetospheric dynamics. A central question to be answered through chaos theory is how far the transition of the magnetospheric system from quiet state to the growth phase and subsequently to the explosive phase of substorms corresponds to a transition from a simple attractor to a chaotic or strange attractor..." (Pavlos, 1988).

The first simple mathematical model for magnetospheric chaos was given by Baker et al. (1990), based on the leaky faucet model in analogy with the work of Shaw (1984). Klimas et al. (1991) extended the Baker dripping faucet model in terms of the geometry and plasma contents of the magnetotail. Experimental evidence for magnetospheric chaos has been found by chaotic analysis of the magnetospheric index *AE* or *AL* measured time series (Vassiliadis et al., 1990; Roberts et al., 1991; Shan et al., 1991). In these studies the main tool for chaotic analysis was the computation of the correlation integral in the reconstructed phase spaces by using the algorithm of Grassberger and Procaccia (1983) according to the

1 Introduction

Magnetospheric dynamics and particularly magnetospheric substorms are associated with the energy transfer from the solar wind to the magnetosphere and subsequently to the ionosphere/atmosphere. The energy coupling between solar wind, magnetosphere and ionosphere constitutes a complex nonlinear process, with strong mass-energy interaction. It is important to note here that the coupling between various subsystems of the global geospace system (near solar wind - magnetosphere - ionosphere) could be understood as a synergetic self-organized holistic system. In this case the coupling of subsystems may be not only energetic (local interactions), but it may include an "informational" (non-local) aspect (Pavlos, 1988; Vörös, 1991). In synergetic theory the "informational" process corresponds to the complementarity between forces and correlations (Nicolis and Prigogine, 1988). The motor machine of the "informational" process could be the slaving principle according to which the physical systems develop order parameters as collective (unstable) modes (Haken, 1988; Doering

Takens embedding theory (Takens, 1981). The above experimental analysis of time series showed that magnetospheric dynamics could be modelled as a chaotic dynamics on a low dimensional strange attractor structure. The weak point however in these experimental results about magnetospheric chaos is that they don't give any support of pseudo-chaotic (low dimensional) profiles of colored noises or self-affine fractional Brownian signals, studied by Osborne and Provenzale (1989) and Provenzale et al. (1992). In previous studies by Pavlos et al. (1992a, 1992b) an extended series of tests was first used in order to exclude the pseudo-chaos of colored noises and afterwards strong evidence for low dimensional magnetospheric chaos was found. Moreover, according to Theiler (1991) the concept of fractal dimension can be applied to time series in two quite distinct ways, the first one to indicate the degrees of freedom in the underlying dynamical system and the second to quantify the self-affinity or "crinkliness" of the trajectory through the phase space. Vassiliadis et al. (1992) followed Theiler's test to surrogate magnetospheric data. In this case when the Theiler parameter w becomes comparable to the autocorrelation time the scaling of correlation integral disappears and there is no convergence of the correlation dimension.

In our previous work (Pavlos et al., 1992a, 1992b) we applied chaotic analysis for two different kinds of magnetospheric time series. First for the auroral electrojet index (*AE* index) measured by ground magnetometers located roughly along the auroral oval. Second, for magnetic field measurements obtained in situ in the plasma sheet of the earth magnetotail. Concerning the use of the *AE* index as a representative measure of global magnetospheric activity, one has to confront the limitations of the index (e.g. Kamide and Akasofu, 1983); still, *AE* is the only routinely available activity estimate with reasonable time resolution. Furthermore, the auroral electrojet index represents the energy dissipation at the auroral ionosphere, which is a crucial variable in the internal dynamics of the magnetosphere, and the cross-scale coupling within the solar wind-magnetosphere-ionosphere system (Daglis et al., 1992, 1994).

In this work, we extend the chaotic analysis for the magnetospheric time series (especially the *AE* index) by using singular value decomposition (*SVD*) analysis according to Broomhead and King (1986). Sharma et al. (1993) have also used *SVD* analysis in the estimation of the eigenvalue spectrum of the *AE* index. We apply *SVD* analysis for the *AE* index time series in combination with Theiler's test in order to discriminate dynamical chaos from self-affinity or "crinkliness". The results of this extended chaotic analysis give strong evidence for magnetospheric chaos especially in relation to the Theiler criterion. Lorenz (1991) has shown that sometimes chaotic analysis based on Grassberger and Procaccia (1983) algorithm can be problematic from a

different point of view than that of colored noises with pseudo-chaos. For this reason, in order to further support the hypothesis of the magnetospheric chaos besides the chaotic analysis of experimental time series we propose a model of magnetospheric chaos by using a nonlinear equivalent magnetospheric electric circuit. A preliminary solution of this model shows that in principle one can support theoretically the above experimental results about magnetospheric chaos.

2 Data analysis

As we show in the next section, it is realistic to suppose that the magnetosphere can be considered as a nonlinear dissipative complex system. In this system some kind of self-organizing process reduces the infinite number of degrees of freedom to a few macroscopic degrees of freedom which describe the dynamics of the system to a low dimensional subspace of the original infinite dimensional phase space. For dissipative systems the volume $V(t)$ enclosed by some closed surface S in the system phase space is known to shrink exponentially in time. In this way the dimensionality is reduced after finite time, and whole sets of solutions may be identified by simple attracting sets, as fixed points, limit cycles or m -dimensional tori, with integer dimension and all Lyapunov exponents negative (or zero). On the other hand systems with dimensionality higher than two, generally have more complicated attracting sets (strange attractors) with one or more positive Lyapunov exponents and fractal of non-integer dimensions. The fractality of the attracting submanifold in the phase space means that the corresponding Hausdorff-Besicovitch dimension and the other generalised dimensions (information dimension, Lyapunov dimension, capacity dimension and correlation dimension) are higher than the topological dimension of the orbit. In realistic cases of dissipative systems the change of control parameters included in the non-linear ordinary differential equations which describe the system dynamics can cause the bifurcation of the system dynamics to different kinds of attractors mentioned above. In the following we use the reconstructed phase space vector

$$R_i = \{x(t_i), x(t_{i+\tau}), \dots, x(t_{i+(m-1)\tau})\} \quad (1)$$

where τ is a delay time. In principle, τ is arbitrary as long as the values $x(t_i)$ and $x(t_{i+\tau})$ are not highly correlated. If τ is too small the coordinates become singular so that $x(t_i) \cong x(t_{i+1})$. If τ is too big, chaos makes $x(t_i)$ and $x(t_{i+(m-1)\tau})$ causally disconnected by amplification of noise. In practice τ is chosen by trial and error searching for optimal results. This reconstructed phase space is used in order to test the existence of the strange attractor as well as to calculate its correlation dimension, along with the largest Lyapunov exponent of the dynamical flow.

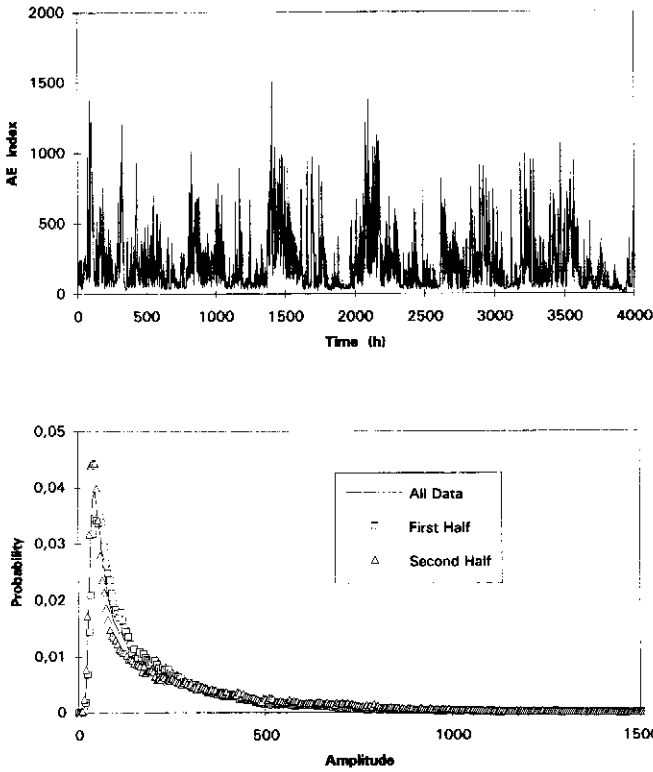


Fig. 1. a. Hourly mean value of AE index time series measured with 1-min time resolution, b. Probability density function of AE index for the entire time series (solid line), the first half and the second half of it.

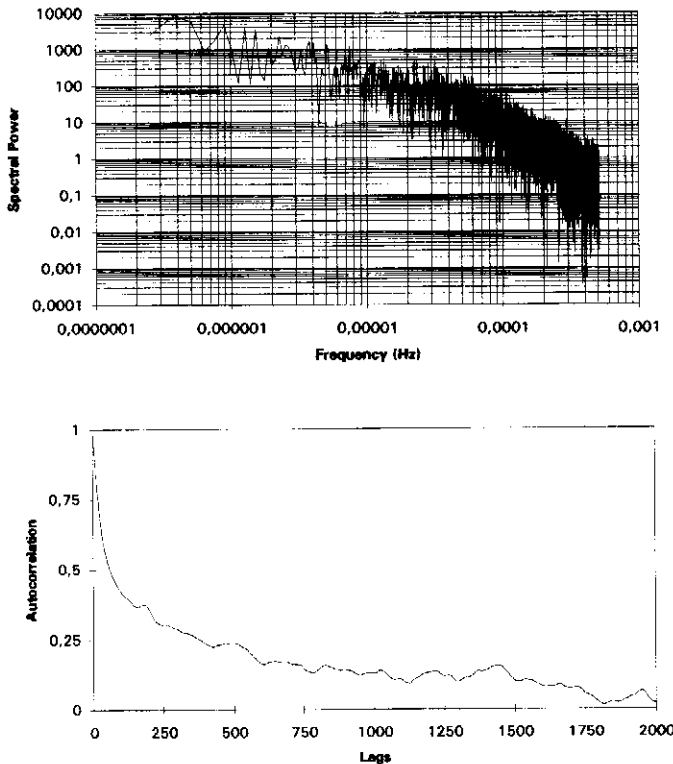


Fig. 2. a. The power spectrum of the AE index time series, b. The autocorrelation coefficient of the AE index times series.

The correlation integral $C(r, m)$ is given by the relation,

$$C(r, m) = (N(N-1)/2)^{-1} \sum_{i=1}^{N-1} \sum_{j=i+1}^N \Theta(|R_i - R_j| - r) \quad (2)$$

where Θ is the Heaviside function and $|R_i - R_j|$ denotes the distance between the states R_i and R_j in the m -dimensional reconstructed phase space. The correlation dimension D of the reconstructed m -dimensional orbit is given by Grassberger and Procaccia (1983):

$$D = \lim_{\substack{r \rightarrow 0 \\ m \rightarrow \infty}} (d \ln C(r, m) / d \ln(r)) \quad (3)$$

When the orbit evolves on a strange attractor manifold then the slope in a log-log plot of the correlation integral $C(r, m)$ in its scaling region, where $C(r, m) \sim r^{d(m)}$, must saturate at a final fractal value D as the embedding dimension m increases. According to an embedding theorem by Whitney (1936), the minimum dimension m_0 of an Euclidean space R^m in which we can find a smooth embedding of the attractor, is $m=2D+1$. Moreover, according to Broomhead and King (1986) qualitative information from the experimental time series may be extracted by using singular value decomposition analysis (SVD). In this analysis the number of degrees of freedom in the $N \times m$ trajectory matrix X , including the phase space vectors $R(t_i)$, leads to the singular value problem:

$$XC = S\Sigma \quad \text{and} \quad X^T S = C\Sigma \quad (4)$$

where $\Sigma = \text{diag}(\sigma_1, \sigma_2, \dots, \sigma_m)$ is the matrix of singular values of X and the columns of C , $\{C_i\}$ ($i=1, \dots, m$) are the singular vectors associated with $\{\sigma_i\}$. The singular vectors $\{C_i\}$ are also eigenvectors of the $m \times m$ covariance matrix $\Xi = X^T X$ of the time series. Since the $\{\sigma_i\}$ are the root mean square projection of the trajectory onto the basis vectors, we would expect that the number which is non-zero is the number of degrees of freedom. According to Broomhead and King (1986) experimental noise which generates spurious degrees of freedom is identified as a noise flood in the singular value problem. This implies partitioning of the embedding space into a d -dimensional deterministic subspace and its orthogonal complement, that is a noise dominated subspace of dimension $m-d$. After this, the use of the $N \times d$ reduced trajectory matrix X with rows

$$\hat{X} = (X_1^T C_1, X_1^T C_2, \dots, X_1^T C_D)^T \quad (5)$$

corresponds to rejection of the out-of-band noise.

Figure 1a shows a part of the time series corresponding to AE index measured with one-minute time resolution. These measurements correspond to the first 2500 hours of the year 1978. During this period were observed more than 3000 substorm events. According to the magnetospheric chaos hypothesis, every substorm must correspond to a close return in the magnetospheric strange

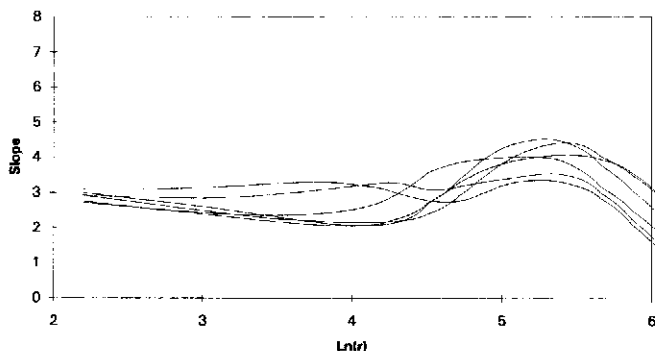


Fig. 3. Slopes $d(m)=d\ln C(r,m)/d\ln(r)$ for embedding dimension $m=8$ and delay times $\tau=20, 50, 100, 200, 300$ and 500 ; the number of samples used were 50000. The best scaling is observed for $\tau=100$.

attractor. Figure 1b shows the probability density function of the *AE* index time series for the entire series, the first half and the second half of it. The form of these density functions in combination with the corresponding mean values and standard deviations show the stationarity of the time series which is a necessary condition in order to have the time series corresponding to the dynamic evolution on a strange attractor. The random character of the *AE* time series is revealed by the broadband form of the power spectrum (Fig. 2a) and the abruptly decaying autocorrelation function (Fig. 2b) revealing a first abrupt delay at the zero during the first 2000 minutes of lag time. The strong decorrelation of the *AE* index signal after 20 units of lag time indicates that the delay time for the phase space reconstruction (according to (1)) must be chosen in this region.

Figure 3 shows the slopes $d_m=d\ln C(r,m)/d\ln(r)$ for $m=8$ and delay times $\tau=20-500$. For $\tau > 20$ there is an apparent plateau ($d_m=\text{constant}$) for low values of distance r in phase space, indicating scaling $C(r;m)\sim r^{d(m)}$ of the estimated correlation integrals. The wavy profile of the slopes reveals that time related phase space vectors R_i were included for the estimation of the correlation integrals. Also for $\tau > 20$ we have about the same value of the slopes at the scaling region. According to Theiler (1991), the concept of fractal dimensions can be applied in two quite distinct ways to the time series analysis. First to indicate the number of degrees of freedom in the underlying dynamical system, and second to quantify the self-affinity or "crinkliness" of the trajectory in the reconstructed phase space. In the second case, more crucial than the high frequency crinkles is whether or not the trajectory is recurrent through phase space. For a non-recurrent colored noise the dimension of the full trajectory will be equal to the dimension of a local segment, while for a recurrent colored noise (if the time series is long enough to be recurrent) the estimated correlation dimension will be that of the embedding space. For chaotic analysis of experimental time series the first case (dynamical fractality) is of interest.

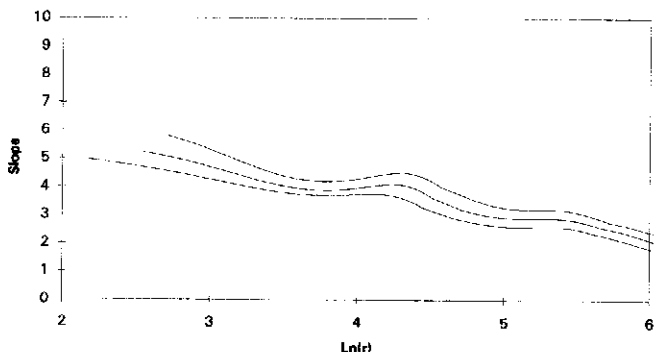
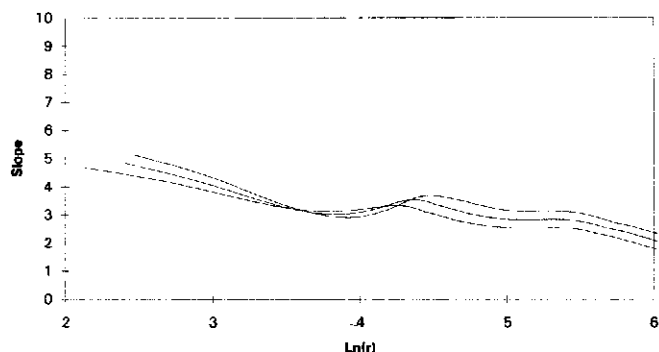


Fig. 4. a. Slopes $d(m)$ corresponding to the Theiler test for embedding dimensions $m=7, 8$ and 9 ; the used delay time is $\tau=100$ units and the Theiler parameter is $w=20$. b. Same as (a) with $\tau=100$ and $w=500$.

For this reason we restrict the sums in equation (2) to i, j pairs in such a way that $|i - j| > w$, for values of w higher than the decorrelation time of the time series. This means that we exclude all the correlated pairs included in a sphere with diameter $2w$.

Figures 4a and 4b show the slopes $d(m)$ for embedding dimensions $m=7, 8$ and 9 , delay time $\tau=100$ and for the Theiler parameter $w=20$ and $w=500$ respectively. As it is shown in Fig. 4, after the exclusion of temporal correlated points on the reconstructed trajectory there is no clear scaling and no clear convergence of the scaling exponent $d(m)$. This means that if the *AE* index time series is connected with low dimensional dynamics then a noisy component in the signal covers the dynamical structure. In order to reduce the noise effect we follow the *SVD* analysis. According to Broomhead and King (1986) all the qualitative information about the dynamical system confined to the deterministic subspace can be extracted from the reduced trajectory matrix X . This amounts to averaging out the high frequency noise contributions in the trajectory. In the following we use the principal components corresponding to the reduced trajectory X in order to estimate the slopes $d(m)$ of the correlation integrals. Also we restrict the estimation of the correlation integrals corresponding to the reduced trajectory, to i, j pairs with $|i - j| > w$, in order to exclude time correlated pairs.

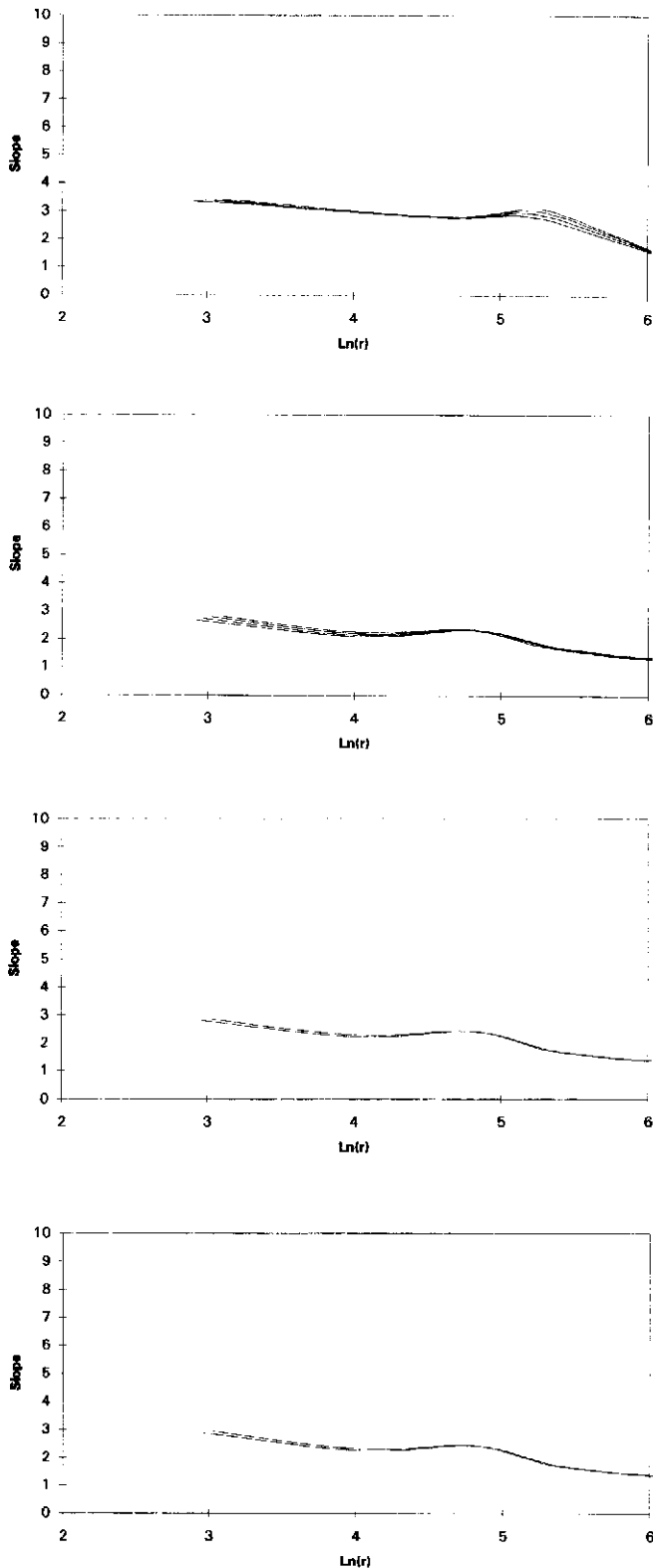


Fig. 5. a. The slopes $d(m)$ ($m=6,7,8,9$), estimated by using the SVD analysis to obtain the reduced trajectory X , for $\tau=20$ and $w=20$. The length of the time series was $N=150000$.
 b. Same as (a) for $\tau=20$, $w=20$ and $N=50000$.
 c. Same as (b) for $w=300$ and $m=7$ and 8 .
 d. Same as (c) for $w=500$.

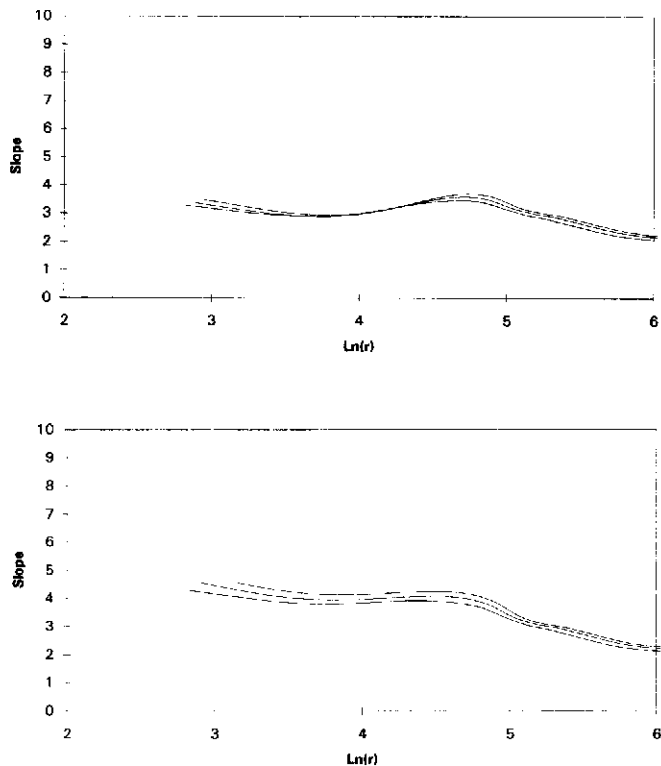


Fig. 6. a. Same as Fig. 5a for $N=50000$, $\tau=100$, $w=20$.
 b) Same as (a) for $w=500$.

Figure 5a shows the slopes $d(m)$ of the reduced trajectories corresponding to $w=20$ and delay time $\tau=20$ units. In this case, slopes for embedding dimension $m=6,7,8$ and 9 reveal a clear scaling of the correlation integrals at low values of r and saturation at a value for $D=3-4$. The length of N of the used time series for the estimation of the correlation integrals was 150000 samples. Figure 5b shows the slopes $d(m)$ for the same parameters $w=20$ and $\tau=20$, but for time series length $N=50000$. The saturation value in this case is a little lower at a value $D=2-3$. For time series length $N>50000$ samples the slopes remain independent of N . Figures 5c and 5d show the slopes $d(m)$ for $m=7$ and 8 , delay time $\tau=20$, and $w=300$ and 500 respectively. The saturation value in both cases remain at the same value $D=2-3$, i.e., appears independent of the parameter w . In order to study the dependence of the slopes upon the delay time we have estimated them for delay times $\tau=100$ and $\tau=500$, also for $w=20$ and $w=500$. The case shown in Fig. 6a ($\tau=100$ and $w=20$), indicates a clear saturation value at $D=3-4$. In the case of Fig. 6b ($\tau=100$, $w=500$), there is only a tendency for saturation in the region of D between 4 and 5 .

Figure 7 shows the slopes $d(m)$ ($m=7,8$ and 9) for $\tau=500$ and $w=500$, which reveal a tendency for saturation at values $D \geq 6$. This result is expected as the noise reduction by SVD analysis can be occurred in an appropriate window length $\tau_w = m\tau \leq \tau_w^*$, where $\tau_w^* = 2\pi/\omega^*$ is the band-limiting frequency. For our data this

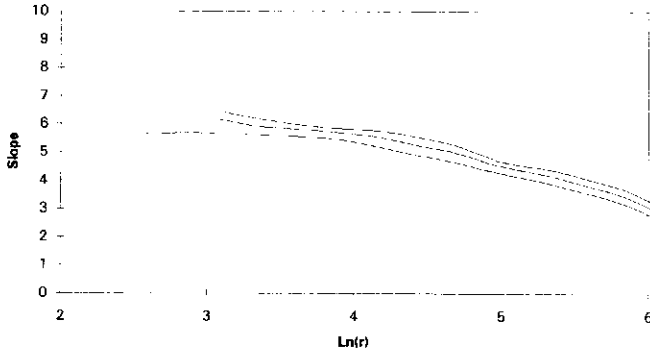


Fig. 7. Same as Fig. 6 for $\tau=500$, $w=500$ and $m=7, 8$ and 9 .

constraint implies that the appropriate delay time τ for the noise reduction is in the range of 50 to 100 units.

The above results support the fractal nature of the phase space trajectory which is due to “close returns” in phase space as the underlying dynamics of the magnetospheric system evolves on the supposed magnetospheric strange attractor.

In the following we use some tests which can exclude the case of pseudo low-dimensional chaos related to colored noises. Provenzale et al. (1991) have shown that time series generated by linear or nonlinear stochastic processes can reveal pseudo chaotic profile. In the case of stochastic processes the saturation of the scaling exponent $d(m)$ seems to be forced by the shape of the power spectrum. This is consistent with the fact that both the power spectrum and the correlation integral are related to the second moments of the distribution. In contrast, for an aperiodic signal corresponding to the motion on the strange attractor, the phase coupling and the phase correlation must play an essential role. Thus, when we randomize the Fourier phase of a stochastic signal $X(t_i)$, the saturation value D of the scaling exponent $d(m)$ must remain the same with the saturation value of the original signal. Conversely, for a random signal $X(t_i)$ corresponding to motion on a strange attractor, the randomization of the phases φ_k of the Fourier representation of the time series,

$$X(t_i) = \sum_k C_k \cos(\omega_k t_i + \varphi_k) \quad (6)$$

must cause drastic changes to the saturation value of the scaling exponent.

Figure 8a shows the slopes $d(m)$ ($m=6, 8$ and 9) estimated from the phase-randomized *AE* index time series. It is apparent that there is no scaling of the correlation integrals and no saturation of their slopes, while the strong wavy profile of the slopes reveal time correlated pairs (R_i, R_j) , included in the estimation of $C(r, m)$. Figure 8b shows the slopes $d(m)$ ($m=6, 8$ and 9) for the phase randomised data corresponding to the correlation integrals which have been estimated after restriction to i, j pairs with $|i - j| > w$ and $w=20$ units. As

it is shown in this figure the exclusion of time correlated pairs implies a clear scaling character, while there is no low dimensional saturation. The same result was obtained for the slopes $d(m)$ estimated by using the reduced trajectory matrix X , obtained by the application of *SVD* analysis at the phase randomised *AE* index time series as it is shown in Fig. 8c.

The above analysis gives strong evidence for the existence of low-dimensional chaotic dynamics in the magnetospheric system. Especially the combination of the *SVD* analysis with the Theiler test showed that the supposed magnetospheric attractor must have a dimension D lower than 4. According to Whitney (1936) these results imply that the magnetospheric dynamics must be smoothly embedded in $(2D+1)$ dimensional phase space with $2D+1=9$ degrees of freedom. This is in accordance with the normalised singular spectra obtained by the *SVD* analysis of the *AE* index shown in Fig. 9. In this figure we can observe that the singular spectrum decreases for embedding dimension $m \leq 12$, while for $m > 12$ it reaches a noise floor.

3 Modeling Magnetospheric Chaos

The experimental estimation of the correlation D by following the Grassberger and Procaccia (1983) algorithm, presupposes that the fine structure of the attractor would on magnification resemble the coarse structure obtained by the reconstruction based on a time series with finite length N . So that if N were made large enough, the decrease of $C(r; m)$ with τ , when τ is very small would be similar to that when τ is fairly large. According to Lorenz (1991), although this demonstrates the case for some simple systems, it is not valid for more intricate ones, including some systems in which certain subsets of the variables are only weakly coupled to others. Lorenz showed that if the variable selected for chaotic analysis (trajectory reconstruction and estimation of the correlation dimension) is strongly coupled to only a few variables of the system, the estimated value of D , if N is only moderately large, will be considerably less than the dimension as determined by other standard methods, such as the Kaplan-Yorke formula. In order to support the low dimensional magnetospheric chaos hypothesis against this negative proposition, we use two critical elements in our analysis. The first is that our results presented above for the correlation dimension are independent from the length of the time series N for $N > 5 \times 10^4$. The second element is the proposition of a nonlinear model for the magnetospheric dynamics.

We now present some concepts that can theoretically support the possibility for the existence of magnetospheric chaos. Lorenz (1963) showed that under certain physical restrictions the partial differential equations which describe a hydrodynamic system (Navier-Stokes equations, the equation for heat conduction and

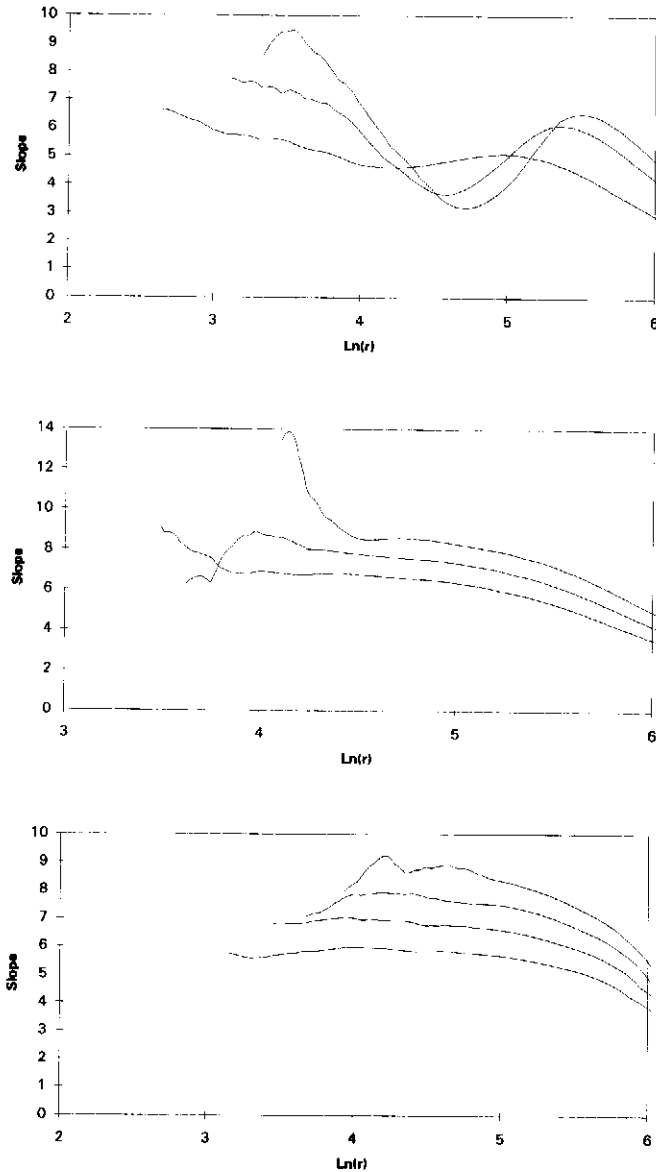


Fig. 8. a. The slopes $d(m)$ ($m=6,8,9$) for the phase randomised AE index with $N=32000$ and $\tau=20$.
 b. Same as Fig. 4 for the phase randomised AE index for $N=32000$, $\tau=20$ and $w=20$.
 c. Same as Fig. 5 for the phase randomised AE index and $\tau=20$, $w=20$.

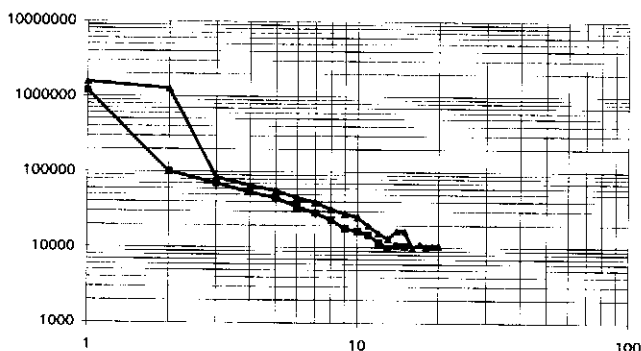


Fig. 9. The singular spectra for the embedding dimensions 15 and 20.

the continuity equation) can be simplified to a set of a three coupled ordinary differential equations. These equations constitute the Lorenz model and can be put in the form

$$\frac{d\bar{X}}{dt} = F(\bar{X}, \sigma, \rho, b) \quad (7)$$

where σ , ρ and b are the control parameters. It is known that this model describes the dynamic evolution of the system state in a three-dimensional phase space. For certain values of the control parameters the motion becomes highly erratic along an unstable manifold known as Lorenz strange attractor. The concept of strange attractor was used by Ruelle and Takens (1971) for explaining the onset of turbulence and nonperiodicity or irregularity observed experimentally in hydrodynamic or atmospheric dissipative systems.

Moreover, it is not out of reality to suppose that the nonperiodicity observed in different space plasma systems is caused by the system's deterministic dynamic evolution along a strange attractor manifold of low dimensionality. In the case of space plasma the hydrodynamic equation for the velocity field will need to be altered to account for Lorenz force experienced by moving charges in electromagnetic fields and Maxwell's equations must be considered to get a closed system of equations. Theoretical and experimental studies showed that MHD systems can reveal chaotic dynamics (see Bhattacharjee (1987)). Truncated equations derived for MHD systems have been used to describe nonperiodic phenomena in solar plasma (Weiss et al., 1984) as well as in magnetospheric convection dynamics (Summers and Mu, 1992). In the study by Summers and Mu (1992) a technique of Fourier analysis followed by a three-mode truncation was applied to MHD equations and was shown that the corotating convection model of the Jovian magnetosphere can be described by equations similar to Lorenz equations which lead to the existence of a magnetospheric strange attractor. Therefore is realistic to claim that the dissipative system of the earth's magnetospheric plasma is possible to show chaotic dynamics.

In the following we suppose that an appropriate nonlinear electric circuit model of the magnetospheric dynamics is physically equivalent to truncated MHD equations corresponding to the magnetospheric plasma system. For the MHD modeling of the magnetospheric dynamics, especially during substorms, refer to Vasyliunas (1975) and Terasawa (1983). According to Liu et al. (1988), the global magnetospheric equivalent electric circuit shown in Fig. 10 consists of :

1. The dynamo region in the magnetotail which generates the cross-tail potential drop Φ_{CT} . This potential can be approximately given by

$$\Phi_{CT} = B_n V_{SW} L_W, \quad (8)$$

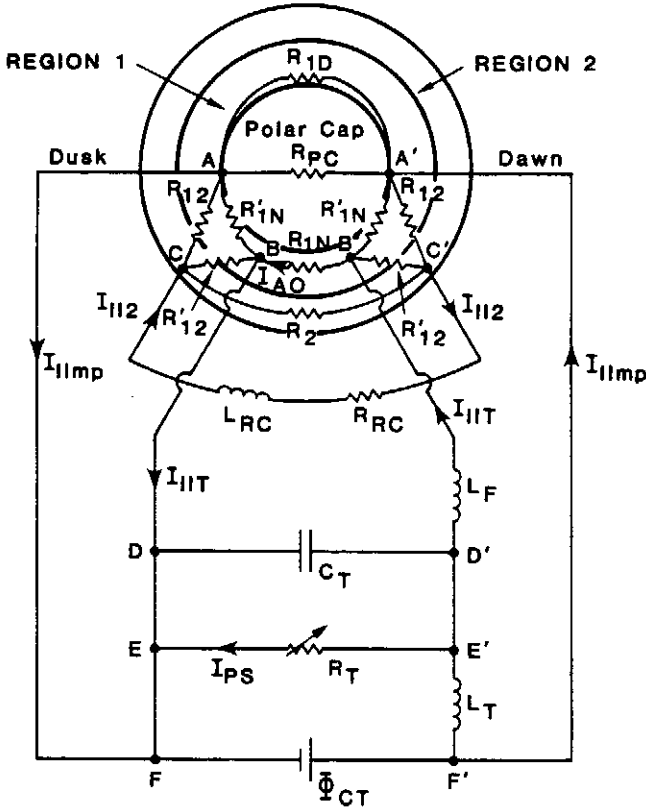


Fig. 10. The magnetospheric equivalent circuit which consists of the magnetotail circuit (Φ_{CT} , L_T , R_T , C_T , L_F), the inner magnetospheric ring current circuit (R_{RC} , L_{RC}) and the polar ionospheric current (R_{1N} , R'_{12} , R_{12} , R_{PC}) (Liu et al., 1988).

where B_n is the normal component of the interplanetary magnetic field, L_w is the width of the open magnetotail and V_{sw} is the solar wind speed Lee and Roederer (1982). During quiet times Φ_{CT} is 20 KV, while during substorms increases to $\cong 100$ -150 KV.

2. The magnetotail circuit, which contains the tail inductance L_T , the field-aligned inductance L_F , the plasma sheet resistance R_T and the magnetotail capacitance C_T .

3. The polar ionospheric circuit, which contains the resistances $R_{PC} \cong 1$ ohm, $R_{1D} \cong 0.8$ ohm, $R_{1N} + R'_{1N} \cong 0.5$ ohm, $R_{12} \cong 0.025$ ohm and the resistance R_2 ($\gg R_{12}$, R_{1N}) taken to be infinite, and

4. The ring current circuit which contains the resistance $R_{RC} \cong 0.02$ ohm and the inductance $L_{RC} \cong 80$ H.

The Liu et al. (1988) equivalent circuit is clearly a linear system because the circuit dynamical elements L_T , R_T , C_T , L_F and R_{1N} are considered to be invariable during the substorm process. The effective magnetotail inductance can be related to the magnetic energy stored in the lobes by the following expression:

$$L_T I_T^2 / 2 = \int_{V_T} (B_T^2 / 2\mu_0) dV_T \quad (9)$$

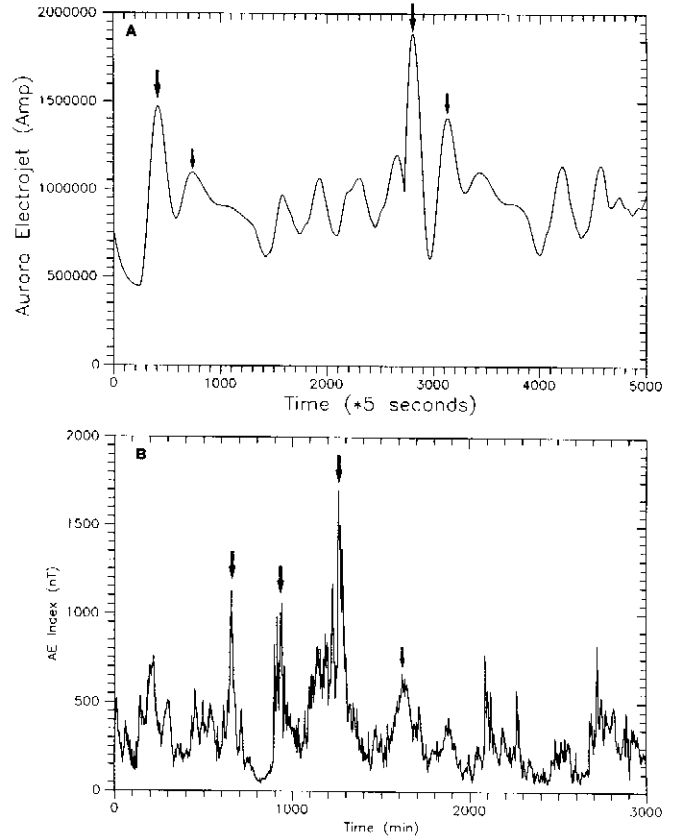


Fig. 11. a. Time profile of the current I_{AO} along the nightside auroral oval. b. AE index showing a variety of substorm events.

Using Ampere's Law $\nabla \times B = \mu_0 J$ for the magnetotail, we can show that $B_T \cong \mu_0 I_T / L_T$ for the magnetic field of the magnetotail and that $L_T \cong \mu_0 L_Y L_Z / L_X$ for the effective inductance, where L_Y , L_Z and L_X are the characteristic lengths of the magnetotail. For the effective capacitance C_T we can obtain an estimate from the magnetotail capacitor stored energy which is equal to the total convective energy in the plasma sheet, that is

$$C_T V_c^2 B^2 L_Y^2 / 2 = m_P N_0^2 V_c L_X L_Y L_Z / 2 \quad (10)$$

where B is the magnetic field in the plasma sheet, L_x , L_y , L_z , are the characteristic lengths of plasma sheet, m_p is the proton mass and $N_0 \cong 0.1 - 1 \text{ cm}^{-3}$ is the plasma density. This leads to the following relation for the effective capacitance

$$C_T = m_P N_0 L_X L_Y / L_Z B^2 = \frac{M_{ps}}{L_Y^2 B^2} \quad (11)$$

where M_{ps} is the total plasma mass in the plasma sheet.

During magnetospheric substorms the plasma sheet resistance R_T changes drastically as a function of the plasma sheet electric current. Microinstabilities driven by crossfield currents can create plasma turbulence and

anomalous transport coefficients such as resistivity, viscosity, diffusion, heat conduction etc. (Papadopoulos, 1980). Moreover, other kinds of instabilities as collisional and collisionless tearing-mode instability (Zelenyi and Taktakishvili, 1987), or nonlinear particle dynamics (particle chaos) in the Earth's magnetotail (Büchner and Zelenyi, 1987; Burkhart and Chen, 1991; Dusenbery et al., 1992; Chen, 1992) can create macroscopic dependence of the plasma sheet resistance R_T on the plasma sheet electric current I_{ps} . According to these theoretical concepts we suppose that the plasma sheet current I_{ps} increases with the strengthening of the cross-tail potential drop Φ_{CT} which can happen after drastic changes of the solar wind parameters (McPherron, 1979; Akasofu, 1981). The increase of the plasma sheet current causes anomalous resistivity and enhancement of the plasma sheet resistance, which in turn causes reduction of the plasma sheet current and current interruption in the tail with simultaneous, sudden injection of the tail current to the nightside ionosphere. We suppose that a possible macroscopic modeling of this process is given by the relations

$$\begin{aligned} \frac{dR_T}{dt} &= \rho_1 < 0, \quad \text{for } \frac{dI_{ps}}{dt} > 0 \\ \frac{dR_T}{dt} &= \rho_2 > 0, \quad \text{for } \frac{dI_{ps}}{dt} < 0 \end{aligned} \quad (12)$$

In addition the effective capacitance C_T and inductance L_T cannot be invariable during magnetospheric substorms, because the characteristic lengths L_X , L_Y , L_Z for the plasma sheet and the magnetotail change drastically. The value of the magnetic field, especially in the plasma sheet, changes too during substorms. The plasma sheet mass M_{ps} increases and the plasma sheet magnetic field B decreases during the substorm recovery and growth phase ($dI_{ps}/dt > 0$), while during the substorm expansion phase ($dI_{ps}/dt < 0$) the inverse changes take place. Changes in the effective capacitance C_T are modeled by the equations

$$\begin{aligned} \frac{dC_T}{dt} &= c_1 > 0, \quad \text{for } \frac{dI_{ps}}{dt} > 0 \\ \frac{dC_T}{dt} &= c_2 < 0, \quad \text{for } \frac{dI_{ps}}{dt} < 0 \end{aligned} \quad (13)$$

Also we suppose that the effective inductance L_T increases during the recovery and growth phase ($dI_{ps}/dt > 0$) as the magnetotail expands, and decreases during the substorm expansion phase ($dI_{ps}/dt < 0$), when a large part of the magnetotail is destroyed.

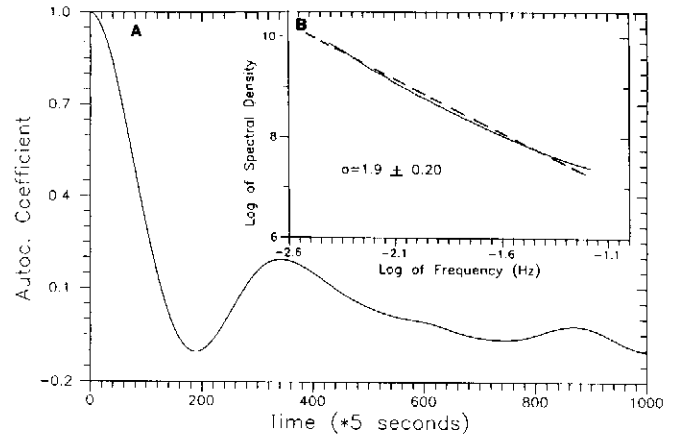


Fig. 12. a. The I_{AO} autocorrelation function. b. Spectral density of the I_{AO} time series.

$$\begin{aligned} \frac{dL_T}{dt} &= \lambda_1 > 0, \quad \text{for } \frac{dI_{ps}}{dt} > 0 \\ \frac{dL_T}{dt} &= \lambda_2 < 0, \quad \text{for } \frac{dI_{ps}}{dt} < 0 \end{aligned} \quad (14)$$

By using phenomenological values for the characteristic lengths L_X , L_Y , L_Z and the magnetic field B of the magnetotail and the plasma sheet we found that the absolute values of the parameters $\rho_{1,2}$ are 2.5 Ohm/h and 12.4 Ohm/h, the absolute values of $c_{1,2}$ are $2 \cdot 10^3$ F/h and 10^4 F/h and the absolute values of $\lambda_{1,2}$ are 50 H/h and 250 H/h.

The above non-linear extension of the magnetospheric electric circuit model of Liu et al. permits to express the general mathematical equations for the magnetospheric system as follows :

$$\frac{d\bar{X}(t)}{dt} = N[\bar{X}(t), \lambda] + \bar{F}(t), \quad (15)$$

where $\bar{X}(t) = (R_T, L_T, C_T, I_T, V_{CT}, I_F, I_{AO})$ represents the magnetospheric circuit state vector and $\bar{F}(t)$ describes the external disturbance of the magnetosphere by the solar wind system. Here the external variable corresponds to magnetospheric dynamo Φ_{CT} . By N we symbolize the nonlinear circuit equations as they result from Kirchoff laws. In general the term $\bar{F}(t)$ makes the system to be non autonomous. Such systems can also reveal chaotic dynamics (Hasler, 1987; Haken, 1988; Brindley and Kapitaniak, 1991; Dykman et al., 1991) or hyperchaos (Arecchi, 1988). Moreover, according to the theory of non autonomous dynamical systems, the potential drop Φ_{CT} can be taken as one further dynamical variable of the magnetospheric system. In accordance to this, Vassiliadis et al. (1993) have included solar wind magnetic field (B_{south}) measurements (B_{south} is related to Φ_{CT} according to (8)) for a 3-D phase reconstruction of the magnetospheric dynamics. In the work of Vassiliadis et al., the magnetospheric dynamics is modeled

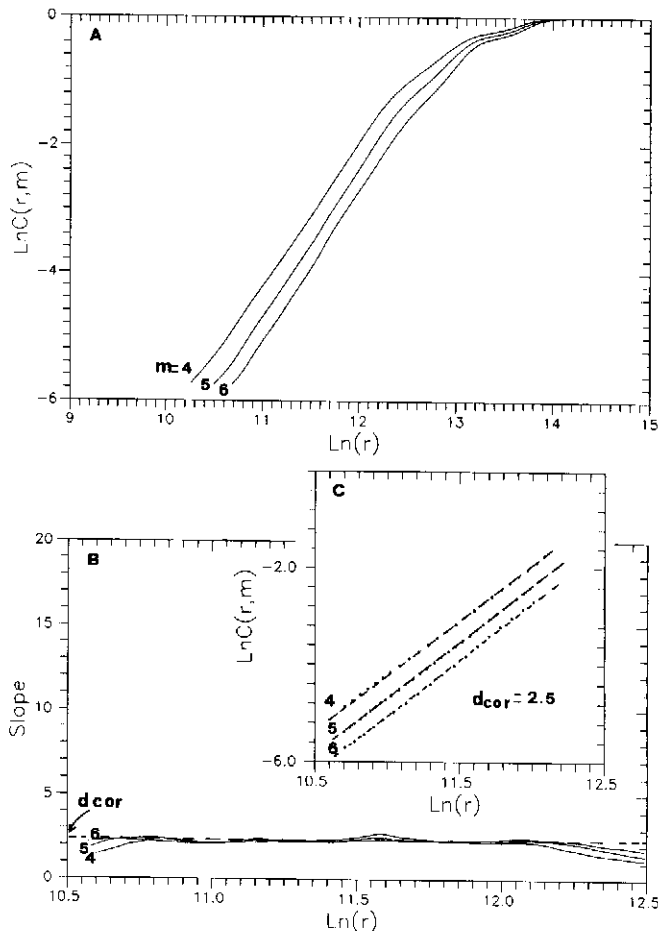


Fig. 13. a. Spectral density of the IAO time series.
 a. The integral correlation function $c(r,m)$ for phase space dimensions $m=4,5,6$.
 b. The slopes $d\ln(C(r,m))/d\ln(r)$ versus $\ln(r)$ are shown for $m=4,5$ and 6.
 c. Linear fitting at the scaling region of the curves.

by a simple linear LRC circuit with constant R, L, C elements. Furthermore, the external disturbance $\bar{F}(t)$ is possible to be considered as the input in an input-output system which can reveal chaos too (Casdagli, 1992; Vasiliadis and Daglis, 1993, 1994).

As a first step in the numerical solution of our model we consider the potential drop Φ_{CT} to be an external control parameter of the magnetospheric system. The value of Φ_{CT} during quiet periods is known to be typically 20KV and 100-150 KV during substorms. By using these values of Φ_{CT} we can obtain the first numerical solution of nonlinear magnetospheric circuits during substorms. In particular we begin with a magnetosphere being in a quiet state ($\Phi_{CT}=20$ KV) and afterwards we disturb the system by a sudden increase of the cross-tail potential drop to the value of 150 KV. This corresponds to a strengthening of the solar wind dynamo. Figure 11a shows one numeric solution $I_{AO}(t)$ which corresponds to AE index in the real magnetospheric system. For comparison of the model with the real system in Fig. 10b

we show typical AE index measurements. The numeric solution shows substorm events (abrupt increases in the AE index) every 1-4 hours which is very near to the real AE index profile. The aperiodic character of the model solution is revealed by the power spectrum and the autocorrelation function of the I_{AO} time series shown in Fig. 12.

Furthermore we use the complete numeric solution $X(t)$ of the model in order to reconstruct the phase space of the system and estimate the correlation dimension of the dynamical trajectory. Fig. 13 presents the correlation integrals and the corresponding slopes which at the scaling region shows saturation of the scaling exponent at the value $D_{\text{cor}} \cong 2.3$. This result is in good agreement with the value of D obtained by chaotic analysis of the real AE index time series. Also the proposed 7-dimensional phase space

$$X(t) = \{R_T, L_T, C_T, I_T, V_{CT}, I_F, I_{AO}\}$$

is in accordance with the low dimension obtained by the experimental singular spectra using the SVD analysis for the AE index shown in Fig. 9. Although a complete study of the nonlinear circuit model proposed above and solved numerically must be done extensively in the future, especially with different mathematical forms for the solar wind disturbance $F(t)$, we believe that the above results constitute a strong evidence for magnetospheric chaos.

4 Summary and Discussion

In the present work chaotic analysis was extended by using SVD analysis in relation with critical tests for the distinction between low dimensional dynamical chaos and pseudochaotic profiles of fractal time series with strong time correlations. This extended chaotic analysis showed that the magnetospheric dynamics must be related with a low dimensional strange attractor with correlation dimension $D \cong 2-4$. Moreover we have presented some theoretical concepts which support the magnetospheric chaos by extending Lorenz theory to magnetised plasmas. Also we used the global magnetospheric equivalent electric circuit in order to specify the order parameters of the magnetospheric dynamics. The numerical solution of the proposed model was found to be in very good agreement with the results of the extended chaotic analysis applied to experimental magnetospheric time series. Of course, the search through of the solution of the nonlinear magnetospheric circuit on the external disturbance must be done in the future, while such a wider study can be used for obtaining methods of predicting the magnetospheric substorms.

Acknowledgements. The authors wish to thank T. Araki and T. Kamei for the supply of 1-min AE index tapes. Also, the authors would like to express their gratitude to the referees for their helpful and constructive suggestions.

References

- Akasofu, S.-I., Energy coupling between the solar wind and magnetosphere, *Space Sci. Rev.*, *28*, 121–190, 1981.
- Arecchi, F. T., Instabilities and chaos in lasers: Introduction to Hyperchaos, in *Order and Chaos in Nonlinear Physical Systems*, pp. 193–224. Plenum, New York, 1988.
- Baker, D. N., Klimas, A. J., McPherron, R. L., and Büchner, J., The evolution from weak to strong geomagnetic activity: an interpretation in terms of deterministic chaos, *Geophys. Res. Lett.*, *17*, 41–44, 1990.
- Bhattacharjee, J. K., *Convection and chaos in fluids*. World Scientific, Singapore, 1987.
- Brindley, J. and Kapitaniak, T., Existence and characterization of strange nochaotic attractor in nonlinear systems, *Chaos, Solitons and Fractals*, *1*, 323–337, 1991.
- Broomhead, D. S. and King, G. P., Extracting qualitative dynamics from experimental data, *Physica D*, *20*, 217–236, 1986.
- Büchner, J. and Zelenyi, L., Stochastic mechanism for the disruption of energy buildup in the magnetospheric tail, *Sov. J. Plasma Phys.*, *13*(2), 102–104, 1987.
- Burkhart, G. P. and Chen, J., Differential memory in the Earth's magnetotail, *J. Geophys. Res.*, *96*, 14,033–14,049, 1991.
- Casdagli, M., A dynamical system approach to modeling input-output systems, in *Nonlinear Modeling and Forecasting*, vol. XII of *SFI Studies in the Sciences of Complexity*, edited by M. Casdagli and S. Eubank, pp. 265–282. Addison-Wesley, New York, 1992.
- Chen, J., Nonlinear dynamics of charged particles in the magnetotail, *J. Geophys. Res.*, *97*, 15,011–15,050, 1992.
- Daglis, I. A., Sarris, E. T., Kremser, G., and Wilken, B., On the solar wind-magnetosphere-ionosphere coupling: AMPTE/CCE particle data and the AE indices, in *Study of the Solar-Terrestrial System, ESA SP-346*, edited by J. J. Hunt and R. Reinhard, pp. 193–198. ESA/ESTEC, Noordwijk, Netherlands, 1992.
- Daglis, I. A., Livi, S., Sarris, E. T., and Wilken, B., Energy density of ionospheric and solar wind origin ions in the near-Earth magnetotail during substorms, *J. Geophys. Res.*, *99*, 5691–5703, 1994.
- Doering, C. R., Gibbon, J. D., Holm, D. D., and Nicolaenko, B., Low dimensional behaviour in the complex Ginzburg-Landau equation, *Nonlinearity*, *1*, 279–309, 1988.
- Dusenbery, P. B., R. F. Martin, Jr., and Burkhart, G. R., Particle chaos in the Earth's magnetotail, *Chaos*, *2*, 427–445, 1992.
- Dykman, G., Landa, P. S., and Neymark, Y. I., Synchronizing the chaotic oscillations by external force, *Chaos, Solitons and Fractals*, *1*, 339–353, 1991.
- Grassberger, P. and Procaccia, I., Measuring the strangeness of strange attractors, *Physica D*, *9*, 189–208, 1983.
- Haken, H., *Information and self-organization*. Springer, Berlin, 1988.
- Hasler, M. J., Electrical circuits with chaotic behavior, *Proc. IEEE*, *75*, 1009–1021, 1987.
- Kamide, Y. and Akasofu, S.-I., Notes on the auroral electrojet indices, *Rev. Geophys. Space Phys.*, *21*, 1647–1656, 1983.
- Klimas, A. J., Baker, D. N., Roberts, D. A., Fairfield, D. H., and Büchner, J., A nonlinear dynamic analogue model of substorms, in *Magnetospheric Substorms, Geophys. Monogr. Ser.*, vol. 64, edited by J. R. Kan, T. A. Potemra, S. Kokubun, and T. Iijima, pp. 449–459. AGU, Washington, D. C., 1991.
- Lee, L. C. and Roederer, J. G., Solar wind energy transfer through the magnetopause of an open magnetosphere, *J. Geophys. Res.*, *87*, 1439–1444, 1982.
- Liu, Z. X., Lee, L. G., Wei, C. Q., and Akasofu, S.-I., Magnetospheric substorms: An equivalent circuit approach, *J. Geophys. Res.*, *93*, 7366–7375, 1988.
- Lorenz, E. N., Deterministic non-periodic flow, *J. Atmos. Sci.*, *20*, 30–141, 1963.
- Lorenz, E. N., Dimension of weather and climate attractors, *Nature*, *353*, 241–244, 1991.
- McPherron, R. L., Magnetospheric substorms, *Rev. Geophys. Space Phys.*, *17*, 657–681, 1979.
- Nicolis, G. and Prigogine, I., *Exploring complexity (An Introduction)*. W. H. Freeman and Company, New York, 1988.
- Osborne, A. R. and Provenzale, A., Finite correlation dimension for stochastic systems with power-law spectra, *Physica D*, *35*, 357–381, 1989.
- Papadopoulos, K., The role of microturbulence on collisionless reconnection, in *Dynamics of the magnetosphere*, edited by S.-I. Akasofu, pp. 289–307. D. Reidel, Dordrecht, 1980.
- Pavlos, G. P., Magnetospheric dynamics, in *Proc. Symposium on Solar and Space Physics*, edited by D. Dialetis, pp. 1–43. National Observatory of Athens, Athens, 1988.
- Pavlos, G. P., Rigas, A. G., Dialetis, D., Sarris, E. T., Karakatsanis, L. P., and Tsonis, A. A., Evidence for chaotic dynamics in the outer solar plasma and the earth magnetosphere, in *Chaotic Dynamics: Theory and Practice*, edited by T. Bountis, pp. 327–339. Plenum, New York, 1992a.
- Pavlos, G. P., Kyriakou, G. A., Rigas, A. G., Liatsis, P. I., Trochoutsos, P. C., and Tsonis, A. A., Evidence for strange attractor structures in space plasmas, *Ann. Geophys.*, *10*, 309–322, 1992b.
- Provenzale, A., Osborne, A. R., Kirwan Jr., A. D., and Bergamasco, L., The study of fluid parcel trajectories in large-scale ocean flows, in *Nonlinear Topics in Ocean Physics*, edited by A. R. Osborne, pp. 367–402. Elsevier, Paris, 1991.
- Provenzale, A., Smith, L. A., Vio, R., and Murante, G., Distinguishing low-dimensional dynamics and randomness in measured time series, *Physica D*, *58*, 31–49, 1992.
- Roberts, D. A., Baker, D. N., Klimas, A. J., and Bargatze, L. F., Indications of low dimensionality in magnetospheric dynamics, *Geophys. Res. Lett.*, *18*, 151–154, 1991.
- Ruelle, D. and Takens, F., On the nature of turbulence, *Commun. Math. Phys.*, *20*, 167–192, 1971.
- Shan, L. H., Hansen, P., Goertz, C. K., and Smith, K. A., Chaotic appearance of the AE index, *Geophys. Res. Lett.*, *18*, 147–150, 1991.

- Sharma, A. S., Vassiliadis, D., and Papadopoulos, K., Reconstruction of low dimensional magnetospheric dynamics by singular spectrum analysis, *Geophys. Res. Lett.*, 20, 335–338, 1993.
- Shaw, R., *The dripping faucet as a model chaotic system*. Aerial Press, Santa Cruz, CA, 1984.
- Summers, D. and Mu, J.-L., On the existence of a Lorenz strange attractor in magnetospheric convection dynamics, *Geophys. Res. Lett.*, 19, 1899–1902, 1992.
- Takens, F., Detecting strange attractors in turbulence, in *Vol. 898 of Lecture Notes in Mathematics*, edited by D. A. Rand and L. S. Young, pp. 366–381. Springer, Berlin, 1981.
- Terasawa, T., Hall current effect on tearing mode instability, *Geophys. Res. Lett.*, 10, 475–478, 1983.
- Theiler, J., Some comments on the correlation dimension of $1/f^\alpha$ noise, *Phys. Lett. A*, 155, 480–493, 1991.
- Vassiliadis, D. and Daglis, I. A., A diagnostic for input-output nonlinear systems: the effect of a nonlinear filter on the correlation dimension, *MPAE-W-100-99-32 report*, 1993.
- Vassiliadis, D. and Daglis, I. A., Developing diagnostics for input-output systems: the effects of certain linear and nonlinear filters on the correlation integral, *Nonlin. Proc. Geophys.*, 1, in press, 1994.
- Vassiliadis, D., Sharma, A. S., Eastman, T. E., and Papadopoulos, K., Low-dimensional chaos in magnetospheric activity from AE time series, *Geophys. Res. Lett.*, 17, 1841–1844, 1990.
- Vassiliadis, D., Sharma, A. S., and Papadopoulos, K., Time series analysis of magnetospheric activity using nonlinear dynamical methods, in *Chaotic Dynamics: Theory and Practice*, edited by T. Bountis. Plenum, New York, 1992.
- Vassiliadis, D., Sharma, A. S., and Papadopoulos, K., An empirical model relating the auroral geomagnetic activity to the interplanetary magnetic field, *Geophys. Res. Lett.*, 20, 1731–1734, 1993.
- Vasyliunas, V. M., Theoretical models of magnetic field line merging, *Rev. Geophys. Space Phys.*, 13, 303–336, 1975.
- Vörös, Z., Synergetic approach to substorm phenomenon, in *Magnetospheric Substorms, Geophys. Monogr. Ser.*, vol. 64, edited by J. R. Kan, T. A. Potemra, S. Kokubun, and T. Iijima, pp. 461–467. AGU, Washington, D. C., 1991.
- Weiss, N. O., Kattaneo, F., and Jones, C. A., Periodic and aperiodic dynamo waves, *Geophys. Astrophys. Fluid Dynamics*, 30, 305–341, 1984.
- Whitney, H., Differential manifolds, *Ann. Math.*, 37, 645–660, 1936.
- Zelenyi, L. M. and Taktakishvili, A. L., Spontaneous magnetic reconnection mechanisms in plasma, *Astrophys. and Space Science*, 134, 185–196, 1987.